Thin-Walled Structures 118 (2017) 46–55

Contents lists available at ScienceDirect

Thin-Walled Structures

journal homepage: www.elsevier.com/locate/tws

Full length article

# Lateral-torsional buckling of fixed circular arches having a thin-walled section under a central concentrated load

Airong Liu[a], Hanwen Lu[a], Jiyang Fu[a], Yong-Lin Pi[b,*]

[a] Guangzhou University-Tamkang University Joint Research Centre for Engineering Structure Disaster Prevention and Control, Guangzhou University, Guangzhou, China

[b] Centre for Infrastructure Engineering and Safety, School of Civil and Environmental Engineering, The University of New South Wales, UNSW Sydney, NSW, Australia

ARTICLE INFO

*Keywords:*
Arch
Axial compression
Bending
Fixed
Lateral-torsional buckling
Rayleigh-Ritz method
Central concentrated load

ABSTRACT

When a thin-walled section arch is subjected to an in-plane central concentrated load, the load produces combined nonuniform axial compressive and bending actions, which increase with an increase of the central load and may reach the values, at which the arch suddenly deflects laterally and twists out of the plane of loading, and fails in a lateral-torsional buckling mode. The elastic lateral-torsional buckling of fixed circular arches under a central concentrated load has been a difficult problem to be solved, which is investigated in this paper. Accurate prebuckling analyses for axial compressive and bending actions produced by the central load are carried out. The analytical solution for the elastic lateral-torsional buckling load is derived using the principle of stationary potential energy in conjunction with the Rayleigh-Ritz method. The analytical solutions for the prebuckling axial compressive and bending actions and for the elastic lateral-torsional buckling load are compared with independent finite element results. It is found that they agree with each other very well, which validate the analytical solutions. In addition, the effects of load height, slenderness and in-plane boundary condition on the lateral-torsional buckling load are investigated. It is found that changes of the slenderness ratio, load height and in-plane boundary conditions have significant effects on the lateral-torsional buckling resistance of arches. This paper provides structural researchers and designers with a deep insight and useful analytical solutions for the lateral-torsional buckling of circular arches, and establishes a sound basis for investigations on the lateral-torsional strengths of fixed circular arches in the future.

## 1. Introduction

The elastic lateral-torsional buckling of pin-ended circular arches that are subjected to nominal in-plane uniform compression or bending moment has been studied extensively, and analytical solutions for the buckling loads have been obtained by a number of researchers [1–13]. Although the lateral-torsional buckling of arches is more complicated than the flexural or torsional buckling of columns and the lateral-torsional buckling of beams due to couplings between the lateral and torsional buckling deformations, a trivial prebuckling stress state was assumed in classical lateral-torsional buckling analyses for such arches, which makes the prebuckling analysis relatively simple [1–13]. In classical analyses, uniform compression in a circular arch is produced by a uniform radial load, while uniform bending is produced by applying equal and opposite bending moment to both ends of a simply supported arch. However, Pi et al. [14–18] found that the stress state in arches subjected to a uniform radial load $q$ is non-trivial. Although the uniform radial load produces a uniform compressive force in a circular arch, its magnitude in shallow arches is much smaller than the trivial value $N=qR$ ($R$ is the radius of the arch) and the bending moment in shallow arches is substantial. When a circular arch is subjected to a central concentrated load, the axial compressive force and bending moment in the arch produced by the load are non-uniform with much more complicated distribution patterns, which makes its lateral-torsional buckling analysis difficult [14–18]. Pi et al. [14–18] investigated the lateral-torsional buckling of out-of-plane pin-ended circular arches that are subjected to a uniform radial load or a central concentrated load and derived an analytical solution for the lateral-torsional buckling load. However, in many cases of engineering practice, both ends of arches are out-of-plane fixed. Lateral-torsional buckling of fixed circular arches under nominal axial compression has been studied in [19–22] by assuming that prebuckling stress state is trivial. Fixed arches under a central concentrated load are subjected to combined axial compressive and bending actions and so the prebuckling stress state is expected to be quite complicated, which have to be considered in the lateral-torsional buckling analysis of fixed arches. In addition, the lateral-torsional buckling mode shape of fixed arches under a central concentrated load is much complicated than that of out-of-plane pin-ended arches. Hence,

* Corresponding author.
*E-mail address:* y.pi@unsw.edu.au (Y.-L. Pi).

http://dx.doi.org/10.1016/j.tws.2017.05.002
Received 13 December 2016; Received in revised form 2 May 2017; Accepted 2 May 2017
0263-8231/

it is difficult to obtain analytical solutions for the lateral-torsional buckling load of fixed arches under a central concentrated load and recourse to numerical methods such as the finite element methods may be made to compute their lateral-torsional buckling loads [23–27]. Analytical solutions for the elastic lateral-torsional buckling load of an arch having out-of-plane fixed boundary condition under central concentrated load and comprehensive investigation of the corresponding lateral-torsional buckling behaviour do not appear to be reported in the literature.

The purpose of this paper is to investigate the elastic lateral-torsional buckling behaviour of fixed circular arches having a thin-walled cross-section under an in-plane central concentrated load. Accurate prebuckling analyses are conducted to determine the distributions of prebuckling axial compressive and bending actions. The correct lateral-torsional buckling mode shape is explored. With the accurate axial compressive and bending actions and the correct lateral-torsional buckling mode shape, the analytical solution for the elastic lateral-torsional buckling load of fixed circular arches is derived. The effects of the in-plane boundary conditions, load height, cross-section and slenderness ratio on the lateral-torsional buckling of fixed arches are also investigated. All analytical solutions are verified by independent finite element results. This paper provides structural researchers and designers with a deep insight and useful analytical solutions for lateral-torsional buckling of circular arches.

## 2. Prebuckling analysis

The fixed circular arch investigated in this paper is shown in Fig. 1, where $R$ is the radius, $S$ the length, $L$ the span, $H$ the rise, and $2\alpha$ the included angle of the arch. The lateral, radial and tangential displacements of the arch axis in the direction $x$, $y$, and $z$ are denoted by $u(\varphi)$, $v(\varphi)$, and $w(\varphi)$, and the twist torsion of the cross-section by $\theta(\varphi)$, where $\varphi$ is the angular coordinate.

Before tackling the lateral-torsional buckling analysis of a fixed circular arch, it is important that prebuckling axial compressive and bending actions in the arch produced by the in-plane central concentrated load (Fig. 1) are correctly determined by an accurate analysis. The differential equations of in-plane equilibrium can be derived by applying the principle of stationary potential energy to the arch and load system. The total potential energy of the system can be expressed as [16,17]

$$\Pi = \frac{1}{2}\int_{-\alpha}^{\alpha}\int_{A} ER\varepsilon^2 dA d\varphi - \int_{-\alpha}^{\alpha}\delta_{\mathrm{D}}(\varphi)QR\tilde{v}d\varphi \tag{1}$$

where $\varepsilon$ is the longitudinal normal strain, $E$ Young's modulus, $A$ the area of the cross-section, $\tilde{v} = v/R$, $\tilde{w} = w/R$, $v$ and $w$ the radial and axial displacements respectively, $()' = d()/d\varphi$, $Q$ the central concentrated load, and $\delta_{\mathrm{D}}(\varphi)$ the Dirac function defined by

$$\delta_{\mathrm{D}}(\varphi) = \begin{cases} +\infty & \varphi = 0 \\ 0 & \varphi \neq 0 \end{cases}, \quad \int_{-\infty}^{+\infty}\delta_{\mathrm{D}}(\varphi)d\varphi = 1 \quad \text{and} \quad \int_{-\infty}^{+\infty}\delta_{D}(\varphi)f(\varphi)d\varphi = f(0) \tag{2}$$

The linear longitudinal normal strain $\varepsilon$ due to in-plane deformations is sufficiently accurate for the prebuckling analysis and has been obtained as [14–18]

$$\varepsilon = \tilde{w}' - \tilde{v} - \frac{y}{R}(\tilde{v}'' + \tilde{w}') \tag{3}$$

Substituting Eq. (3) into Eq. (1) and applying the principle of stationary potential energy, which requires that the first variation of the total potential energy of the system vanishes, lead to

$$\delta\Pi = \int_{-\alpha}^{\alpha}\left[AER(\tilde{w}' - \tilde{v})(\delta\tilde{w}' - \delta\tilde{v}) + \frac{EI_x}{R}(\tilde{v}'' + \tilde{w}')(\delta\tilde{v}'' + \delta\tilde{w}')\right]\mathrm{d}\varphi - \int_{-\alpha}^{\alpha}\delta_{\mathrm{D}}(\varphi)QR\delta\tilde{v}\mathrm{d}\varphi = 0 \tag{4}$$

where $I_x$ is the second moment of area of the cross-section about its major principal axis $ox$ (Fig. 1).

Integrating Eq. (4) by parts obtains

$$\begin{aligned}\delta\Pi = &\int_{-\alpha}^{\alpha}\left\{\left[\frac{EI_x}{R}(\tilde{v}^{iv} + \tilde{w}''') - AER(\tilde{w}' - \tilde{v}) - \delta_{\mathrm{D}}(\phi)Q(R + y_q)\right]\delta\tilde{v} - \left[\frac{EI_x}{R}(\tilde{v}''' + \tilde{w}'') + AER(\tilde{w}'' - \tilde{v}')\right]\delta\tilde{w}\right\}d\phi \\ &+ \left[\frac{EI_x}{R}(\tilde{v}'' + \tilde{w}') + AER(\tilde{w}' - \tilde{v})\right]\delta w\Big|_{-\alpha}^{\alpha} \\ &+ \frac{EI_x}{R}[(\tilde{v}'' + \tilde{w}')\delta\tilde{v}' - (\tilde{v}''' + \tilde{w}'')\delta\tilde{v}]\Big|_{-\alpha}^{\alpha} = 0\end{aligned} \tag{5}$$

The last two terms of Eq. (5) vanish at both ends of the in-plane fixed and pin-ended arches. Hence, for Eq. (5) to be held for arbitrary infinitesimal variations $\delta\tilde{v}$ and $\delta\tilde{w}$, the terms in the brackets of the integration should vanish, which lead to the differential equations of equilibrium for the in-plane deformations of arches as

$$\frac{EI_x}{R}(\tilde{v}^{iv} + \tilde{w}''') - AER(\tilde{w}' - \tilde{v}) - \delta_{\mathrm{D}}(\varphi)Q(R + y_q) = 0 \tag{6}$$

in the radial direction, and

$$\frac{EI_x}{R}(\tilde{v}''' + \tilde{w}'') + AER(\tilde{w}'' - \tilde{v}') = 0 \tag{7}$$

in the axial direction.

For fixed arches, the essential kinematic boundary conditions

$$\tilde{v}' + \tilde{w} = 0, \quad \tilde{v} = 0, \quad \tilde{w} = 0 \quad \text{at} \quad \varphi = \pm\alpha \tag{8}$$

need to be satisfied.

For in-plane pin-ended arches, the essential kinematic boundary

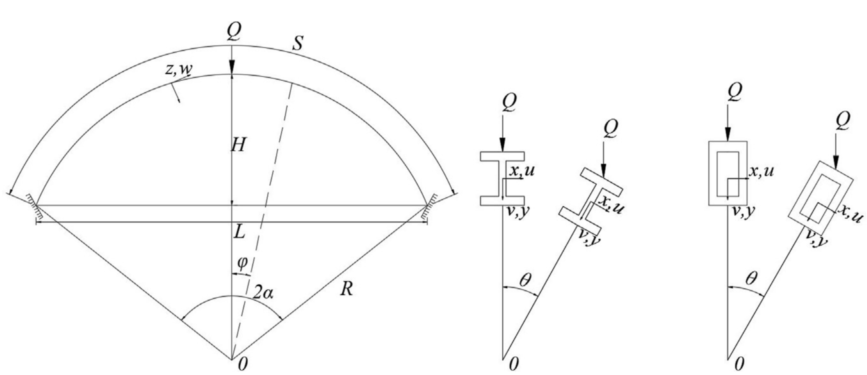

**Fig. 1.** Lateral–torsional buckling.